Proceedings of the Korean Nuclear Society Autumn Meeting
Taejon, Korea, October 2000

Heat Removal Capability Map for Power Reactors During A Core-Melt Accident

Yong-Hoon Kim, Kune Y. Suh, Un Chul Lee, Sang Baik Kim*, Hee Dong Kim*

Seoul National University
San 56-1 Shinrim-dong, Kwanak-gu, Seoul, 151-742, Korea
*Korea Atomic Energy Research Institute
P.O. Box 105, Yusong, Taejon, 305-600, Korea

Abstract

Parametric studies were performed to assess the sensitivity in determining the maximum in-vessel heat removal capability from the core material relocated into the lower plenum of the reactor pressure vessel (RPV) during a core melt accident. A fraction of the sensible heat can be removed during the molten jet delivery from the core to the lower plenum, while the remaining sensible heat and the decay heat can be transported by rather complex mechanisms of the counter-current flow limitation (CCFL) and the critical heat flux (CHF) through the irregular, hemispherical gap that may be formed between the freezing oxidic debris and the overheated metallic RPV wall. It is shown that under the pressurized condition of 10MPa with the sensible heat loss being 50% for the reactors considered in this study, i.e. TMI-2, KORI-2 like, YGN-3&4 like and KNGR like reactors, the heat removal through the gap cooling was capable of ensuring the RPV integrity as much as 30% to 40% of the total core mass was relocated to the lower plenum. The sensitivity analysis indicated that the cooling rate of debris coupled with the sensible heat loss was a significant factor. The newly proposed heat removal capability map (HRCM) clearly displays the critical factors in estimating the maximum heat removal from the debris in the lower plenum. This map can be used as a first-principle engineering tool to assess the RPV thermal integrity during a core melt accident. The predictive model also provided with a reasonable explanation for the non-failure of the test vessel in the LAVA experiments performed at the Korea Atomic Energy Research Institute (KAERI), which apparently indicated a cooling effect of water ingression through the debris-to-vessel gap and the intra-debris pores and crevices.

1. INTRODUCTION

Recent analysis of the TMI-2 reactor accident in 1979 suggested that additional cooling mechanisms not previously considered were present when mostly the oxidic core melt relocated into the water-filled lower plenum of the reactor pressure vessel (RPV) [1]. A cooling mechanism due to boiling in a gap between the debris crust and the RPV wall was proposed for the TMI-2 reactor accident analysis [2-5]. If there is enough heat transfer through the gap to cool the outer surface of the debris and the inner surface of the wall, the RPV wall may preserve its integrity during a core melt accident without needing further cooling of the external surface by flooding of the cavity for instance.

In preliminary LAVA experiments performed at the Korea Atomic Energy Research Institute (KAERI), influence of the internal pressure load on the lower head vessel wall and the material characteristics of the simulant melt on gap formation was systematically investigated as part of the SONATA-IV (Simulation of Naturally Arrested Thermal Attack in Vessel) program [6]. In parallel, VISU experiments at KAERI demonstrated that the heat transfer through the gap was related to the counter-current flow limitation (CCFL) [2]. While relevant experiments are being carried out in the U.S. [7] and Japan [8] as well as domestically to understand the baseline heat transfer mechanism through the multidimensional, irregular, hemispherical, narrow gap of large diameter, the database is still limited and comprehensive mechanistic predictive tools are yet to be developed. On the other hand, external cooling of the RPV has drawn more attention than the complicated in-vessel cooling or gap cooling [9,10]. At the Seoul National University, as an advanced in-vessel design concept, the COASIS (Corium Attack Syndrome Immunization Structures) are being developed as prospective in-vessel retention devices for a next-generation water reactor in concert with existing ex-vessel management measures [11].

If the heat removal through gap cooling in the range of the critical heat flux (CHF) relative to CCFL is pronounced, the safety margin of the reactor can be far greater than what had previously been known in the severe accident management arena. During a severe accident, the RPV integrity may well be maintained because of the potential cooling of the degraded core in a narrow (mm range) gap between the debris crust and the RPV wall. This paper presents the results for maximum heat removal capability in the narrow hemispherical gap for typical Korean nuclear units with thermal output ranging from 2000 to 4000 MWt as well as for LAVA tests in light of the TMI-2 vessel survival. The parametric analysis results indicate that the gap cooling mechanism may take effect in the RPV lower plenum only prior to depressurization of the primary system.

2. MAXIMUM HEAT REMOVAL CAPABILITY

2.1 Material characteristics of debris

2.1.1 Density

In order to investigate the lower head debris behavior in the TMI-2 reactor, thermophysical properties were estimated for the debris on the lower head consisting of a solidified continuous layer covered by a bed of loose debris. Samples of the solidified debris from the hard layer in contact with the lower head, termed companion samples, were extracted from the vessel in order to assess the properties of the melt [12]. Densities of nine companion samples ranged from 7.45 to 9.40 g/cm^3, with an average of 8.4 ± 0.6 g/cm^3. The microstructure observed in the samples indicated an overall composition that was uranium-rich $(U,Zr)O_2$. Radiochemical analyses of the debris indicated that the debris was composed of about 70 w/o U, 13.75 w/o Zr and 13 w/o O. The remaining 3 w/o represented the stainless steel and Inconel constituents that were probably melted during relocation. In the TMI-2 Vessel Investigation Project Integration Report [13], decay heat calculations were performed to estimate the heat generated within the hard layer of debris upon the lower head.

Examinations at the Japan Atomic Energy Research Institute (JAERI) revealed that simulated fuel debris had a chemical composition and density similar to typical TMI-2 debris, and its melting point was measured to be about 2840K [14]. Examinations of the JAERI samples indicated a similar density range from 6 to 8.8 g/cm^3, with an average value of 7.7 g/cm^3. In the current work, a density value of 8.4 g/cm^3 [12] is applied in calculating heat removal from the debris.

2.1.2 Specific heat

The material composition of the TMI-2 debris compound was estimated to be of 78 w/o UO_2 and 17 w/o ZrO_2 weight fraction [13]. Because most material relocated from the core to the lower head vessel had temperatures in the range of 2873K to 3123K [15], the pouring debris must have been between liquid and solid phases. The specific heats for UO_2 and ZrO_2 in the liquid state are 0.502 kJ/kgK and 0.810 kJ/kgK, respectively [16]. Then the specific heat for a 78 w/o UO_2 + 17 w/o ZrO_2 and 80 w/o UO_2 + 20 w/o ZrO_2 compound will be approximately 0.560 kJ/kgK and 0.563 kJ/kgK, respectively.

2.2 Geometric structure of relocated debris

In order to calculate the geometric structure of debris relocated onto the lower plenum, the reactor design parameters and test conditions are needed as collected in Tables 1 and 2.

Figure 1 shows the geometric structure of debris relocated in the RPV lower head specified by

$$Z^3 - 3R^2 Z - \frac{3V}{p} + 2R^3 = 0 \quad (1)$$

From equation (1), the height (H) and the radius (r) of the debris can be determined. Then the surface area of the debris facing the RPV lower head can be computed as

$$S_{side} = pR^2 \sin^{-1}(1) - pZ\sqrt{r^2 - Z^2} - pZ\sqrt{R^2 - Z^2} - pR^2 \sin^{-1}\left(\frac{Z}{R}\right) \quad (2)$$

In all the reactors, the hemispherical RPV lower head is more than enough to contain the whole molten core material. Note that the in-core instrumentation nozzles and other structural materials in the lower plenum are not considered in this calculation. The side area facing the RPV lower head is used to compute the downward heat flux from the debris. It was found that the sensible heat flux from the debris facing the RPV lower head is twice the decay heat flux of debris. The upper surface area can be utilized to determine the upward heat flux from the debris facing the steam-water mixture or the remaining core and the upper plenum structure above. If there exist pores and crevices within the solidified debris, the upward heat flux may increase. Quantitative analysis of intra-debris pores and crevices is not performed in this study, however. Rather, we concentrate on the single heat transfer mechanism in the debris-to-RPV annular gap limited by the CCFL for conservative first-principle estimate of the heat removal capability. From the maximum heat removal point of view, the more the intra-debris pores and crevices, the greater the probability of the RPV survival than by the gap cooling mechanism alone.

2.3 Maximum heat removal requirement

The heat to be removed includes the decay heat released from the radioactive core material and the sensible heat released when the molten core material solidifies in the presence of the coolant. In case of the TMI-2 accident, specific decay heats were calculated at 224 minutes after shutdown, which corresponds to the time that the major relocation of debris to the lower head occurred, and at 600 minutes for the later cooldown period. The decay heat produced from the selected radionuclide inventory was 0.13 W/g of debris (0.18 W/g of U) at 224 minutes and 0.096 W/g (0.14 W/g of U) of debris at 600 minutes after the accident.

Since the debris is rapidly relocated, 50% of the sensible heat is assumed to be released during relocation from the core to the lower plenum. Hence, in order to calculate the heat removal requirement, the sensible heat produced from cooling of the molten core material must be added to the decay heat produced from the radionuclides. On account of the heat transport within the molten pool of debris being governed by natural circulation [17], 30% of the total heat is supposed to be transferred to the lower head vessel wall while the remaining portion is transmitted upward. In fact, the heat removal requirement consists of 30% decay heat plus 30% sensible heat. Only 50% of the total sensible heat is considered to be released from the debris bed in the lower plenum, while the other 50% had already been removed during the relocation process. The sensible heat transfer rate is calculated from the cooling rate and the specific heat as follows.

$$Q_{sensible} = \frac{(1-f)mc_p\Delta T}{\Delta t} \quad (3)$$

Here $\Delta T/\Delta t$ signifies the cooling rate of debris which is a measure of energy release from the molten core material to the coolant. Sensitivity analysis was performed with respect to the sensible heat loss ratio. Results of the analysis are presented in section 3.

2.4 Modeling approach

2.4.1 Assumptions

When the fuel melts and is relocated into the lower plenum, various heat transfer mechanisms can take effect. In general, the relocated material is divided into the metal layer, crust and molten debris pool. For the metal layer, the possibility that the metal layer may stick to the RPV inner wall cannot be totally excluded. However, it is considerably more difficult to examine the heat removal from the gap that may partially be filled with the metal, which lies outside the scope of the present study and thus is not considered here. Figure 2 illustrates various heat transfer mechanisms for the debris cooling within the lower plenum.

For the thermal analysis of degraded core in the RPV lower plenum, it has been widely exercised to consider only two paths of heat transfer, i.e. boiling and radiation at the top surface and conduction through the lower head. If rapid cooling was possible due to water ingress into the gap, the heat transfer phenomena between the debris crust and the RPV deserve the highest attention in the development of maximum in-vessel heat removal capability [6].

Since the heat transfer from cooling the debris takes place in a short period of time, the amount of the sensible heat greatly contributes to the enthalpy. In the TMI-2 accident it is reported that the crust was formed over about 2 minutes. Therefore, the sensible heat corresponding to the amount of 19 tons, which has to be removed in a short period of time, is the heat removal requirement. The assumption used in this study is that all the debris solidifies. In addition, it is reported that the heat flux generated from the debris depends on the vessel angle due to natural convection taking place within the molten pool. In this study, however, it is assumed that there is no heat flux dependency on the vessel angle and that the heat is only removed through the gap between the crust of debris and the RPV wall. At this time, the system pressure is considered to be 10 MPa, and the heat removal through the gap will be dominated by CCFL at the top annular opening between the debris crust and the RPV wall.

The assumptions made in the current modeling are summarized below:

- Superficial velocity of vapor is obtained by the Richter correlation [18].
- Debris is frozen at the top with pancake crust geometry with annular clearance from the RPV wall.
- Heat removal requirement consists of decay heat and the sensible heat.
- Heat is only removed through the narrow annular hemispherical gap between the debris crust and the RPV.
- The accident scenario is similar to that for TMI-2.
- Heat removal through the annular gap is governed by CCFL.

Also, the assumptions made in analyzing the LAVA experiments [19,20] are summarized below:

- The cooling rate of the simulant material was measured to be in the range of 0.8 to 4.0K/s (see Table 3) at the system pressure of 2MPa.
- The gap size is varied as 0.1, 0.3 and 0.5 mm for sensitivity study.

2.4.2 Modeling for maximum heat removal

The continuity equation for the two phases in the upper cross-section in Fig. 2 becomes

$$r_f j_f = r_g j_g \tag{4}$$

The maximum heat removal rate can be calculated from the maximum liquid flow rate through a simple energy balance given by

$$Q_{t,\max} = h_{fg} A_g r_g j_{g,\max} \tag{5}$$

In this equation $j_g^{*1/2}$ =0.4 is applied to obtain $j_{g,\max}$. The correlation for the top flooding is taken from Richter [18].

In this study, since the top flooding behavior in the annuli formed between the debris crust and the vessel wall is of special interest (see Fig. 2(b)), the flooding correlation for annuli of Richter's is introduced as

$$C_w Bo^3 j_g^{*6} S_e^{*2} j_f^{*2} + C_w Bo j_g^{*4} + 150 C_w \frac{j_g^{*2}}{S_e^*} = 0 \tag{6}$$

where $S_e^* = \frac{S}{D_{eff}}$.

For liquid zero penetration, i.e. $j_f^* = 0$, equation (6) can be converted as follows.

$$j_g^{*2} = -\frac{75}{BoS^*}\left[1-\left(1+\frac{BoS_e^{*2}}{75^2 C_w}\right)^{1/2}\right] \quad (7)$$

If the last term in equation (7) is less than unity, the gas velocity for liquid zero penetration is given as

$$j_g^{*1/2} = 0.4 \quad (8)$$

where $j_g^* = j_g\left[\frac{?_g}{D_{eff}\, g(?_f - ?_g)}\right]^{1/2}$, D_{eff} : average circumference of annuli (see Fig. 2(b))

To obtain the gas velocity for liquid zero penetration into a gap, equation (8) is consistently applied in this study. As far as the liquid penetrates, the heat may be removed through the annular gap. While the gas velocity for liquid zero penetration is attained, the heat removal capability is restricted. The average circumference of the annular gap in equation (8) represents the geometric scaling between the prototypic reactor vessel and the smaller test vessel.

Figures 3 through 4 show the heat removal capability for TMI-2 like reactors and LAVA, respectively, utilizing the predictive tool developed in this section.

3. SENSITIVITY ANALYSIS

The sensitivity analyses were performed for four different nuclear power plants. Figure 5 shows the schematic core melt relocation process and its associated sensitivity analysis. Figure 6 presents the sensitivity analysis results for TMI-2 like reactors. The sensitivity study was performed for the following parameters (see Fig. 5).

- Gap size : 0.1, 0.5, 1 and 2 mm.
- Cooling rate: 0.4, 1 and 10 K/s [1]. If the cooling rate exceeds 10 K/s, the RPV will always fail. Hence, the cooling rate in excess of 10 K/s is meaningless from the thermal point of view.
- Sensible heat loss: 10, 30, 50, 70 and 90%. The sensible heat loss refers to heat assumed to be released during relocation from the core to the lower plenum.

Hofmann et al. [15] indicated that a well-mixed (U, Zr)O_2 solid solution, as shown by the metallography and scanning electron microscope results, would be found in a peak temperature range between 2873K and 3123K. Consequently, it was suggested that the peak temperature of the melt relocated to the lower head was at least 2873K. Because of scarcity of data, however, the cooling rate of the debris was not well known. In the meantime Rempe et al. [1] indicated that the cooling rate of the debris was 0.4 ~ 110 K/s, which served as the basis for selecting the range of cooling rates studied in this work.

Each reactor is analyzed with a range of cooling rates at the constant pressure of 10MPa. Results indicate that the maximum heat removal capability is quite sensitive to the cooling rate as expected. If the cooling rate is 10 K/s, the heat released from the molten debris jet during relocation from the core to the lower plenum will rapidly be transferred to RPV so that the RPV is slated to fail. Relevant figures do demonstrate that the RPV failed for all the cases except for the sensible heat loss of 90%.

Since the cooling rate turned out to be a significant factor in determining the maximum heat removal capability, the sensitivity analysis was performed with a constant cooling rate varying the sensible heat loss. However, the sensible heat loss and the cooling rate are rather dependent upon one another. Therefore, the greater the cooling rate, the more the sensible heat loss. Out of cases for the reactor applications, the first case represents the most reasonable case with small sensible heat loss and low cooling rate. Since the first case for each reactor represents a most reasonable case, the maximum heat removal capability is less than 20% of the core inventory at the pressure of 10 MPa. When the debris of less than 20% of the total core inventory is relocated in the lower plenum, the RPV will not fail.

A heat removal capability map (HRCM) is drawn simultaneously accounting for the system pressure, gap size, cooling rate, and sensible heat loss. Figure 7 typically shows the HRCM for the case of TMI-2.

Considering different reactor design parameters, the HRCM can similarly be constructed for KORI-2 like, YGN-3&4 like, respectively. Figures 7 through 10 show the HRCM for each reactor types. The definition for each term used in the HRCM is given below.

- □ $M^* = \frac{M}{M_{Max}}$, M : relocated debris mass, M_{Max}: total core material mass
- □ $P^* = \frac{P}{P_{Max}}$, P : system pressure, P_{Max} : 10MPa (the system pressure during the TMI-2 accident)
- □ $C^* = \frac{C}{C_{Max}}$, C : cooling rate for calculating sensible heat, C_{Max} : 10 K/s (limiting value), C_1^* =0.04, C_2^* =0.1, C_3^* =1
- □ $S^* = \frac{S}{S_{Max}}$, S : sensible heat loss, S_{Max} : maximum sensible heat, S_L^* =0.1, S_M^* =0.9
- □ $E^* = \frac{E}{E_{Max}}$, E : heat removal capability, E_{Max} : maximum heat removal capability for each condition

4. DISCUSSION OF RESULTS

Figures 3 shows the maximum heat removal capability with the gap size of 1 mm, the sensible heat loss of 50%, and the cooling rate of 1 K/s for TMI-2 reactors. The message in these graphs is that as far as the heat removal capability curves lie above the heat removal requirement (i.e., more heat may be removed than is transferred downward to the vessel from the debris) the vessel and the debris may safely be cooled through the gap prior to reaching the flooding limit in the annular passage for the vapor escape and the liquid penetration. Otherwise, the cooling of the debris and the vessel inner wall may not be effective enough to guarantee the lower head integrity from the thermal point of view. When the pressure was 10MPa, the heat removal capability for TMI-2, KORI-2 like, YGN-3&4 like and KNGR like reactors was in the range of 20% to 40% of the total core mass relocated to the lower plenum. If the cooling capability of the intra-debris pores and crevices is comparable to debris-to-vessel gap heat removal capability, heat removal from the debris will be greatly augmented than by the gap cooling alone.

Application of the model to the LAVA experiments demonstrated that the integrity of the vessel filled with preheated water was preserved when the gap size exceeds 0.1 mm, which is consistent with experimental observation as shown in Fig. 4. It is demonstrated that the gap size of 0.1 mm has the marginal heat removal capability region, while the gaps greater than 0.1 mm have the heat removal capabilities always exceeding the heat removal requirement in the thermally safe region. As a matter of fact, the gap size measured or observed from the LAVA experiments was on the order of several millimeters [20]. Results of the analysis for the LAVA experiments in Fig. 4 indicate that when there exists the gap larger than, say 0.1 mm between the debris and the vessel, the vessel can survive the thermal attack from the high-temperature melt.

Pressure, cooling rate and sensible heat loss were found to significantly affect the heat removal capability. Also, the sensible heat will be released during relocation from the core to the lower plenum. In order to calculate the heat removal requirement, the sensible heat produced from cooling of debris must be added to the decay heat produced from the radionuclides. As more sensible heat is lost, more heat removal is required. Sensible heat is a function of the specific heat. Hence, the sensible heat loss actually affects the heat removal capability, which is consistent with the sensitivity analysis results.

Gap size significantly affects the result for LAVA analysis as illustrated in Fig. 4. The effect of gap size in Fig. 6 for the power reactors, however, is shown to be negligible so that the heat removal curves for varying gap sizes are virtually indistinguishable from one another. However, there do exist minor differences as shown enlarged in the Fig. 6 inset. The reason is that if the gap size is of the millimeter order, the physical dimension of the gap clearance is no loner so much important on the heat removal scale of the large power reactors as the existence of the gap itself.

Figure 7 condenses in the HRCM all the information contained in Fig.3 regarding the heat removal capability in the gap versus the total amount of the decay plus the sensible heat that ought to be taken out from the given mass of core material relocated to the lower plenum for the case of TMI-2 as an illustrative example. Critical factors in determining the maximum heat removal capability for the reactor are represented in the non-dimensional parameters already explained in section 3 in light of gap cooling governed by the CCFL through the narrow annular passage shown in Fig. 2. The reference point and the TMI-2 point indicated on curve C_2^* reiterate the maximum heat removal capability versus the requirement and the reactor accident condition shown in Fig. 3. If the TMI-2 accident had taken place at a depressurized condition, the HRCM indicates that the TMI-2 reactor must have failed as illustrated in Fig. 7. Based on the scenario generally known, however, analysis for the TMI-2 accident shows that the reactor was in the Capability Region II in Fig. 7, and thus indeed survived the thermal attack from the relocated core material in accordance with the HRCM. Figures 8 through 10 present the HRCM of KORI-2 like, YGN 3&4 like, KNGR like reactors, respectively.

As the pressure decreases, the vapor escape velocity increases as predicted by the CCFL correlation. The gap cooling is affected by top flooding that is restricted with the pressure. It is shown that the higher the pressure, the greater the heat removal capability in terms of gap cooling within the RPV lower plenum. It is also demonstrated that both the cooling rate and the sensible heat loss as well as the system pressure are the critical factors in assessing the heat removal requirement. It is thus seen that the gap cooling mechanism may only take effect in the RPV lower plenum if the primary system is not depressurized.

5. CONCLUSION

With a number of assumptions and simplifications introduced, we analyzed the maximum heat removal capability through the narrow gap that may be formed during a core melt relocation accident. Parametric studies and sensitivity analyses were carried out for four different nuclear power plants of TMI-2, KORI-2 like, YGN-3&4 like and KNGR like reactors per thermal power output to quantitatively assess the heat removal capability varying the gap size, pressure, cooling rate and the sensible heat loss. Despite certain uncertainties involving the predictive tool developed in this study, our analyses yielded consistent results as to failure or survival of the vessel for different combinations of cooling conditions and the debris mass in the lower plenum in terms of the heat removal requirement versus the maximum heat removal capability for the reactor and LAVA test cases. It was shown that when the pressure was 10MPa with the sensible heat loss being 50% for TMI-2, KORI-2 like, YGN-3&4 like and KNGR like reactors, the heat removal through the gap cooling was effective enough to ensure the RPV integrity as much as 30% to 40% of the total core mass was relocated to the lower plenum. The sensitivity analysis indicated that the primary system pressure and the cooling rate of debris coupled with the sensible heat loss were the significant factors. The newly proposed HRCM displayed in a condensed format the factors of pivotal importance in determining the maximum heat removal capability. This map can be used as the predictive tool in assessing the RPV thermal integrity during a core melt accident.

If the cooling capability of the intra-debris pores and crevices is comparable to debris-to-vessel gap heat removal capability, heat removal from the debris will be greatly augmented than by the gap cooling alone.

REFERENCES

1. J. L. Rempe et al., "Investigation of the Coolability of a Continuous Mass of Relocated Debris to a Water-filled Lower Plenum," *EG&G Idaho Report*, EGG-RAAM-11145 (1994).
2. J. H. Jeong et al., "Experimental Study on CHF in a Hemispherical Narrow Gap," *OECD / CSNI Workshop on In-Vessel Core Retention and Coolability*, Garching, Germany, March (1998).
3. K. Y. Suh and R. E. Henry, "Integral Analysis of Debris Material and Heat Transport in Reactor Vessel Lower Plenum" *Nuclear Engineering & Design*, Vol. 151, No.1, pp. 203-221, November (1994).
4. K. Y. Suh and R. E. Henry, "Debris Interactions in Reactor Vessel Lower Plena During A Severe Accident - I. Predictive Model," *Nuclear Engineering & Design*, Vol. 166, pp. 147-163, October (1996).
5. K. Y. Suh and R. E. Henry, "Debris Interactions in Reactor Vessel Lower Plena During a Severe Accident: II. Integral Analysis," *Nuclear Engineering & Design*, Vol. 166, pp. 165-178, October (1996).
6. K. Y. Suh et al., "Melt Coolability Study Within Hemispherical Vessel Lower Plenum," Submitted for Publication in Nuclear Technology, June (2000).
7. R. E. Henry et al., "An Experimental Investigation of Possible In-vessel Cooling Mechanisms," *CSARP Meeting*, Bethesda, MD, USA, May (1997).
8. Y. Maruyama et al., "In-Vessel Debris Coolability Studies in ALPHA Program," *Proceedings of the International Topical Meeting on PSA'96*, Park City, UT, USA, September (1996).
9. T. G. Theofanous et al., " Critical Heat Flux through Curved, Downward Facing, Thick Walls," *Nuclear Engineering and Design*, Vol. 151, pp. 247-258 (1994).
10. F. B. Cheung and K. H. Haddad, "A Hydrodynamic Critical Heat Flux Model for Saturated Pool Boiling on a Downward Facing Saturated Pool Boiling on a Downward Facing Curved Heating Surface," *Int. J. Heat Mass Transfer*, Vol. 40, No. 6, pp. 1291-1302 (1997).
11. I. S. Hwang et al., "In-Vessel Retention against Water Reactor Core Melting Accidents," Submitted for Publication in *Nuclear Technology*, June (2000).
12. L. A. Stickler et al., "Calculations to Estimate the Margin to Failure in the TMI-2 Vessel," *NUREG/CR-6196*, TMI V(93)EG01, EGG-273 (1994).
13. J. R. Wolf et al., "TMI-2 Vessel Investigation Project Integration Report," *NUREG/CR -6197*, TMI V(93)EG10, EGG-2734 (1994).
14. H. Uetsuka and F. Nagase, "Companion Sample Examination and Related Study by JAERI," *OECD documents*, pp. 269-280 (1993).
15. P. Hofmann et al., "Reactor Core Material Interactions at Very High Temperature," *Nuclear Technology*, Vol. 87, No.1, August (1989).
16. J. K. Hohorst, "SCDAP/RELAP5/MOD2 Code Manual, Volume 4: MATPRO – A Library of Materials Properties for Light-Water-Reactor Accident Analysis," *NUREG /CR-5273*, EGG-2555, February (1990).
17. O. Kymalainen et al., "Heat Flux Distribution from a Volumetrically Heated Pool with High Rayleigh Number," *Proceedings of the 6th Nuclear Reactor Thermal Hydraulics (NURETH 6)*, pp 47-53, Grenoble, France, October 5-8 (1993).
18. H. J. Richter, "Flooding in Tubes and Annuli," *Int. J. Multiphase Flow*, Vol. 7, No. 6, pp. 647-658 (1981).
19. K. H. Kang et al., "Experimental Investigations on In-Vessel Debris Coolability through Inherent Cooling Mechanisms," *OECD/CSNI Workshop on In-Vessel Retention and Coolability*, Garching, Germany, March 3-6 (1998)
20. K. H. Kang et al., "Study on the Melt Relocation Process in the In-Vessel Corium Retention Experiment (LAVA Experiment)," *Proceedings of the Korean Nuclear Society Spring Meeting*, Kori, Korea, May 26-27 (2000).

Table 1. Design Parameters for Reactors Studied

	TMI-2 Reactor	KORI-2 Like Reactor	YGN-3&4 Like Reactor	KNGR Like Reactor
Thermal Power [MWt]	2272	1876	2815	3816
System Pressure [MPa]	15.5	15.5	15.5	15.5
Weight of Fuel Assemblies [ton]	128	73	116	157
Inner Diameter of Vessel [m]	4.43	3.35	4.12	4.74

Table 2. Test Conditions for LAVA (Taken from Reference 20)

Experiment	Melt Composition	Melt Mass [kg]	Subcooling of Coolant [K]	Coolant Level [cm]	Pressure [bar]
LAVA-4	Al_2O_3	30	50	50	17.9
LAVA-5	Al_2O_3	30	22	50	17.9
LAVA-7	Al_2O_3	30	34	50	17.6
LAVA-8	Al_2O_3	30	56	25	16.4
LAVA-9	Al_2O_3	30	24	50	17.0

Table 3. Cooling Rates from LAVA (Taken from Reference 20)

Experiment	Cooling Rate of Simulant Debris [K/s]	Maximum Temperature of Vessel Outer Surface [K]	Cooling Rate of Vessel [K/s]
LAVA-4	1.1	1067	1.3-4.0
LAVA-5	3.9	877	0.3-0.6
LAVA-7	0.8	1164	0.7-1.3
LAVA-8	2.2	1148	0.5-0.8
LAVA-9	4.0	773	2.0

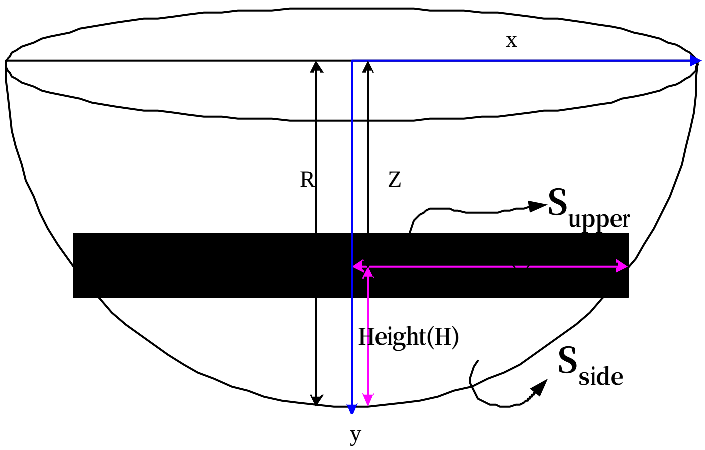

Fig. 1 Hemispherical Geometry of Debris Relocated into the Lower Plenum

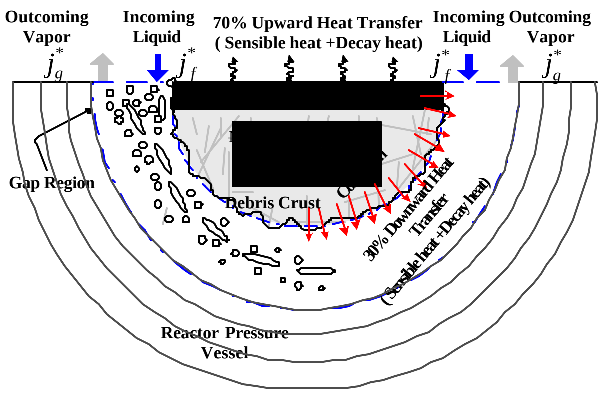

(a) Side View

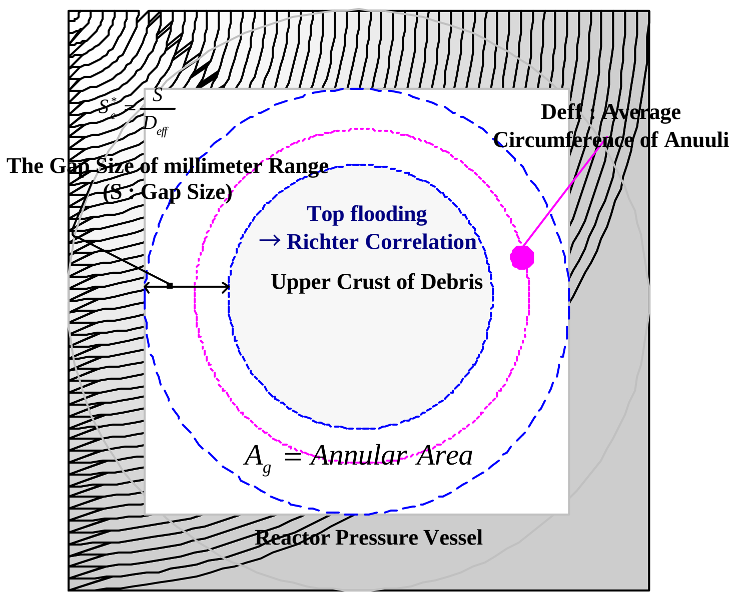

(b) Top View

Fig. 2 Heat Transfer Mechanisms for Debris in the Lower Head

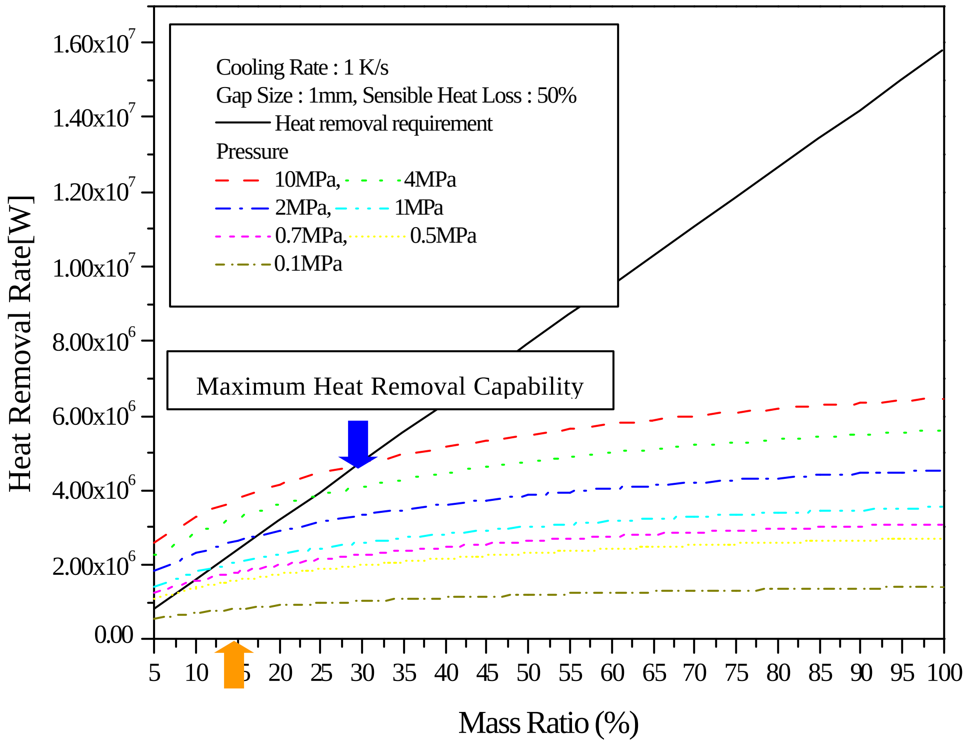

Fig. 3 Maximum Heat Removal Capability by Pressure for TMI-2

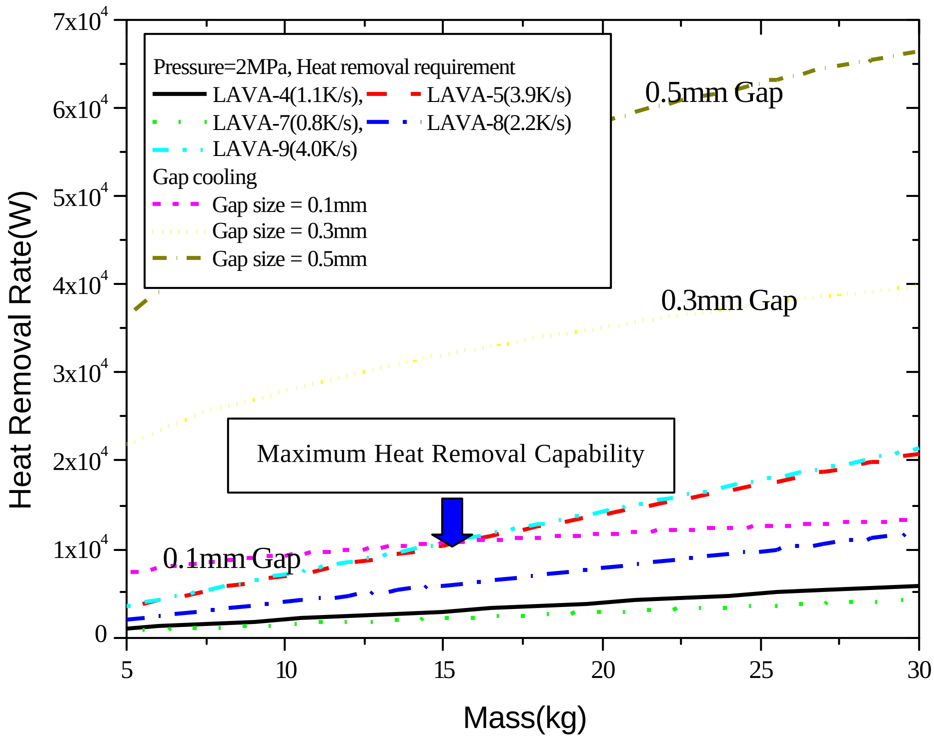

Fig. 4 Maximum Heat Removal Capability by Gap Size for LAVA at 2MPa

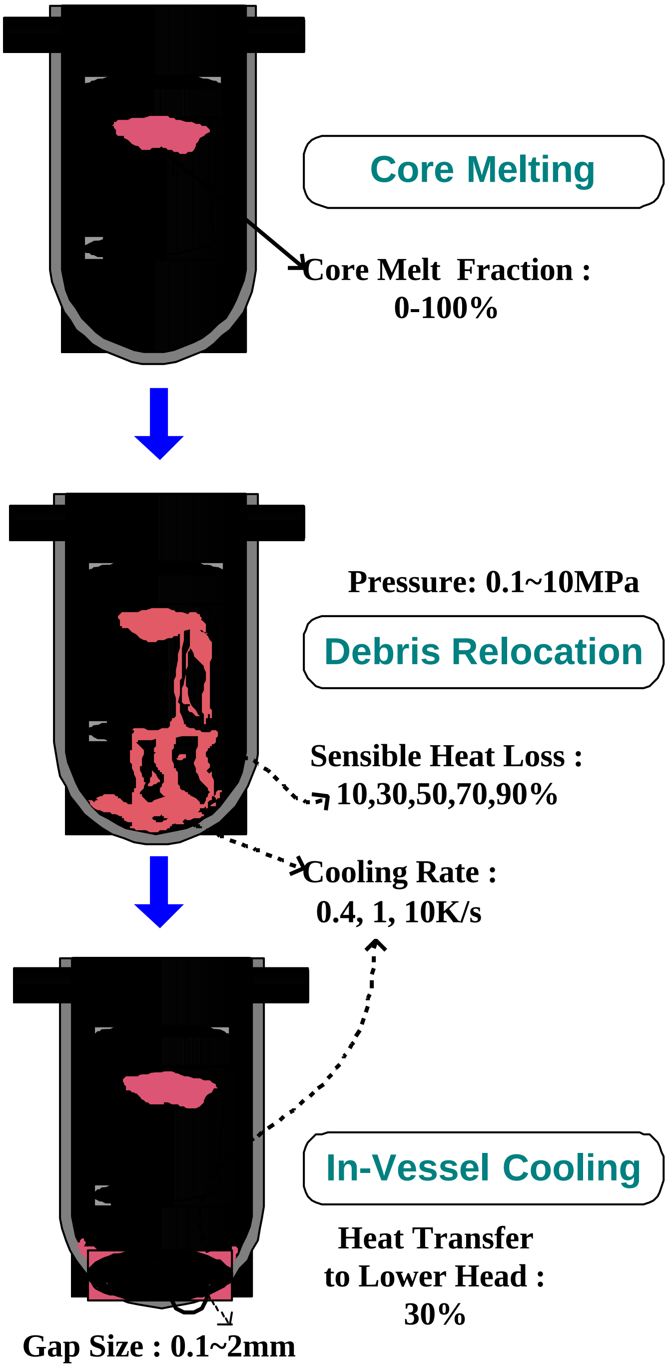

Fig. 5 Core Melt Progression and Parametric Study for Sensitivity Calculation

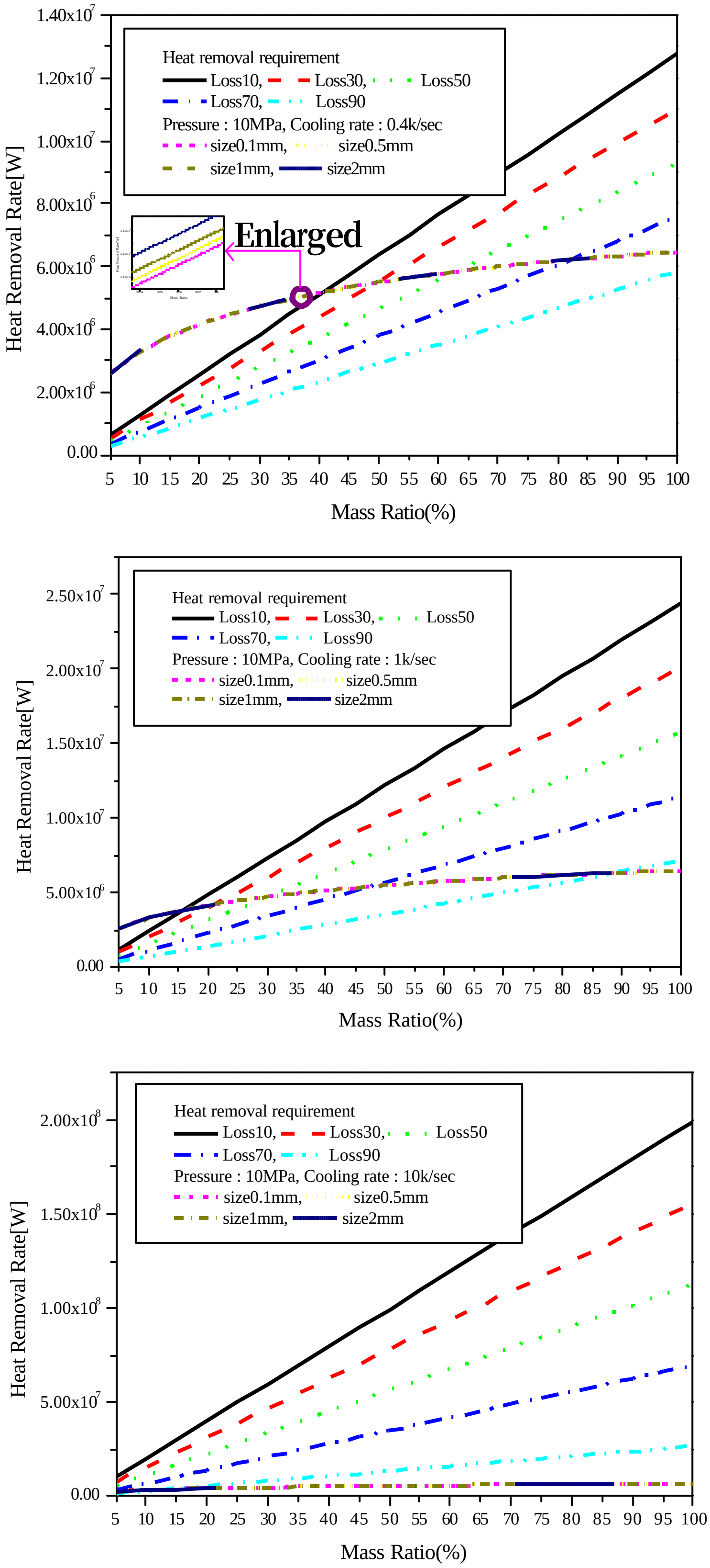

Fig. 6 Sensitivity Analysis for TMI-2

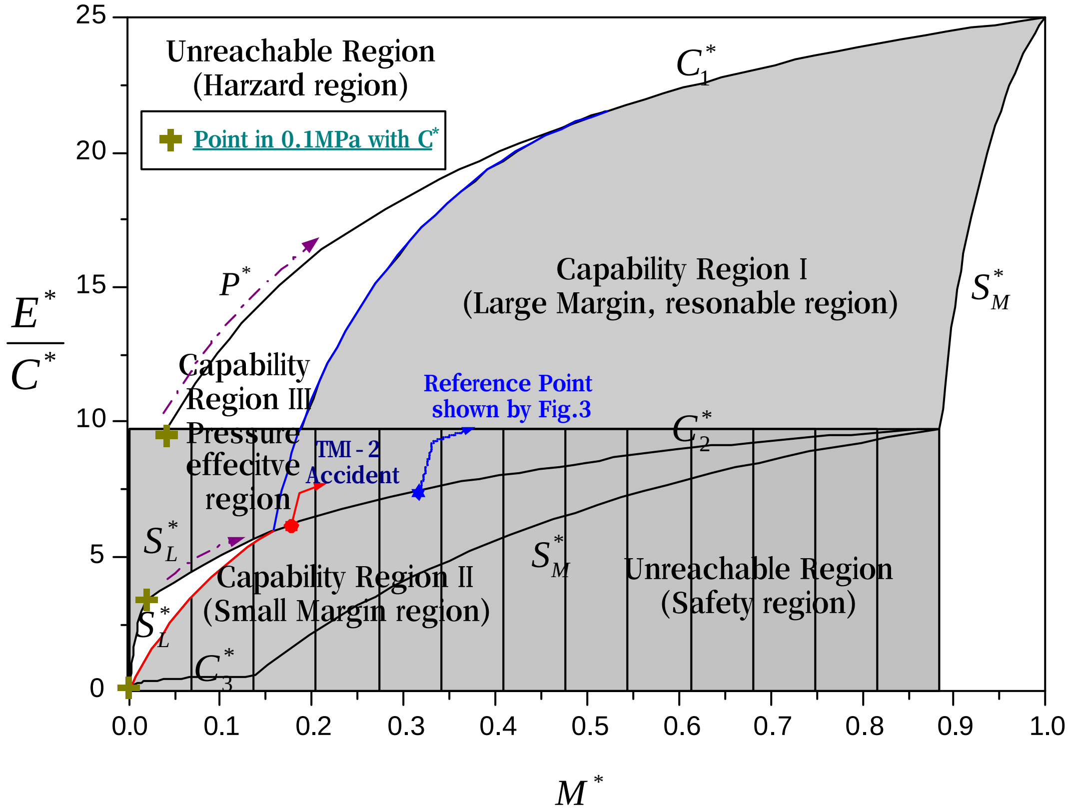

Fig. 7 Heat Removal Capability Map for TMI-2

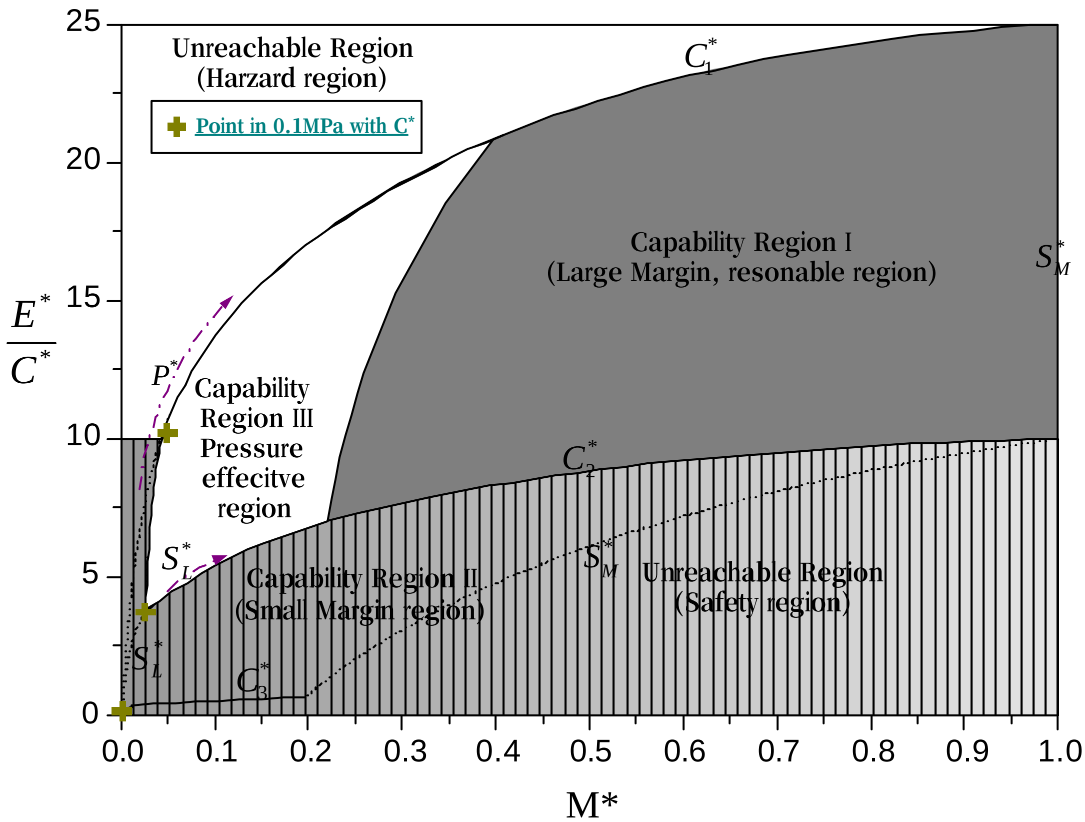

Fig. 8 Heat Removal Capability Map for KORI-2 Like Reactor

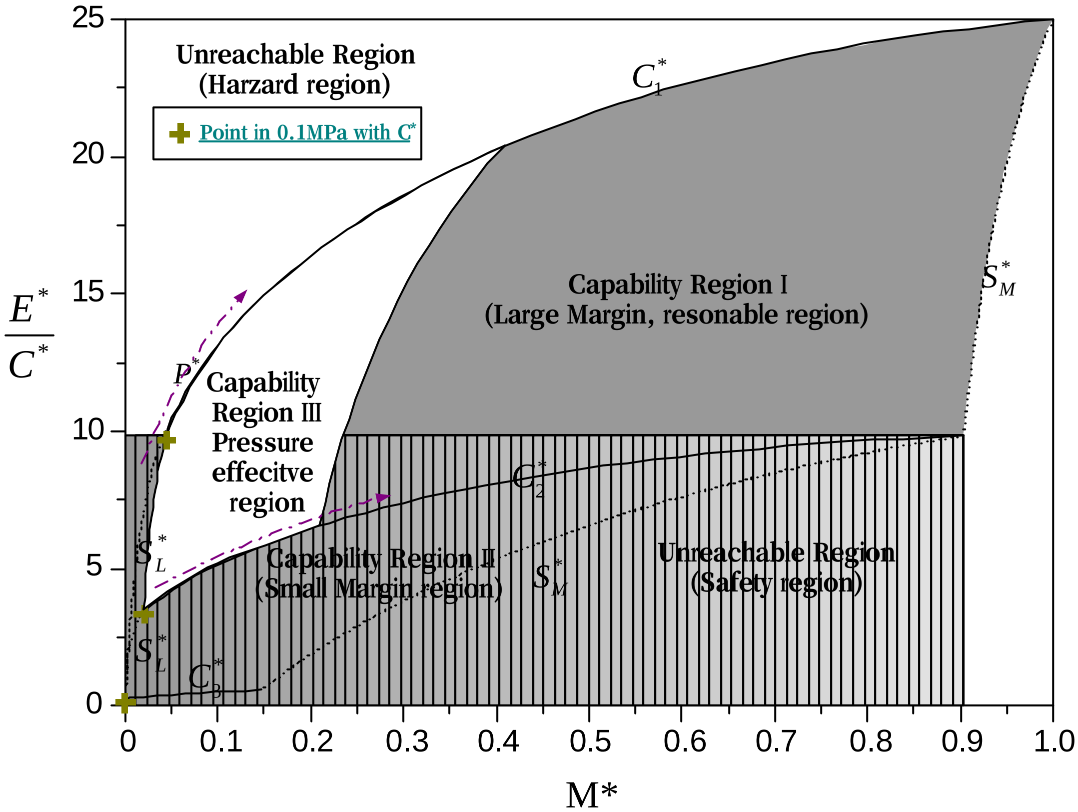

Fig. 9 Heat Removal Capability Map for YGN 3&4 Like Reactor

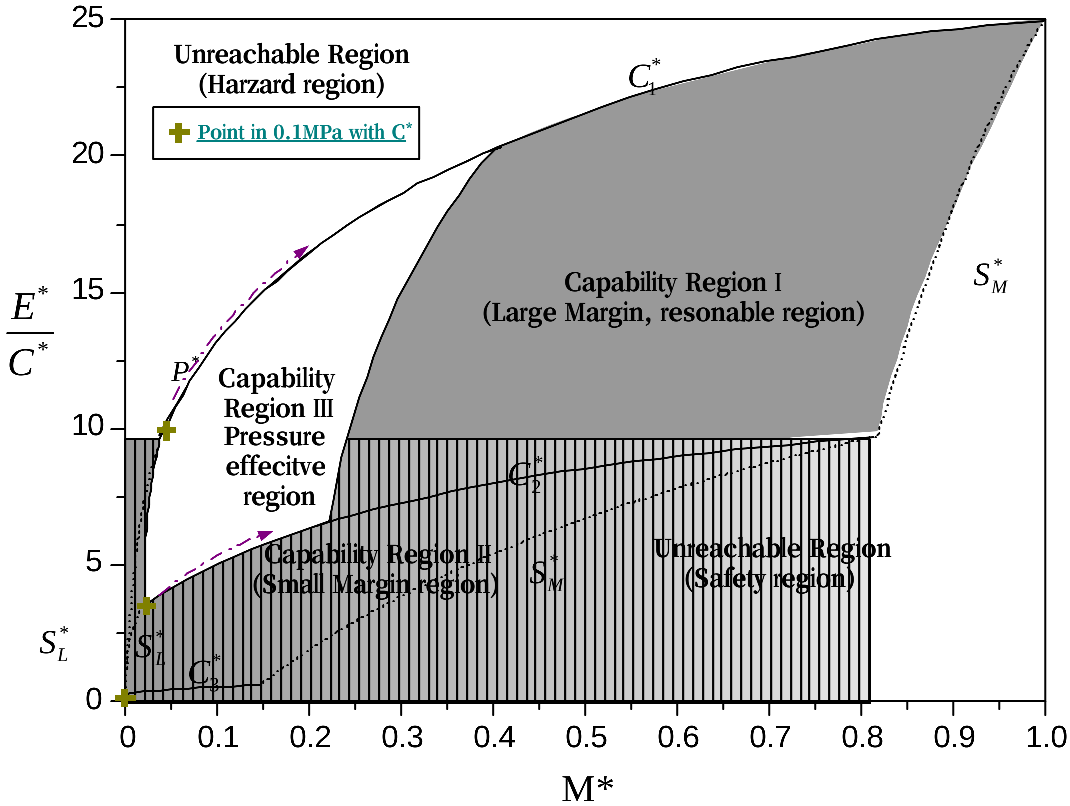

Fig. 10 Heat Removal Capability Map for KNGR Like Reactor